J. Fluid Mech. (1999), *vol.* 385, *pp.* 21–40. Printed in the United Kingdom

© 1999 Cambridge University Press

Curved slender structures in non-uniform flows

By A. R. GALPER AND T. MILOH

Faculty of Engineering, Tel-Aviv University, Israel 69978

(Received 19 February 1998 and in revised form 12 October 1998)

General expressions are derived for the load distribution acting on an arbitrary curved and twisted rigid or deformable slender cylindrical structure moving in an ambient non-uniform potential flow field. Further simplifications are presented for flexible shapes in the limit of a small cross-section. The general analysis is illustrated for straight, toroidal and helical shapes. These shapes are frequently encountered in nature and are good examples of typical fluid–structure interaction problems.

1. Introduction

One of the fundamental problems in fluid mechanics is the computation of the distribution of the hydrodynamic loading along a slender deformable (time-dependent) structure with an arbitrary flexible central line, which is moving relative to an imposed stream. The time-dependent motion of the thin body is generally coupled with the ambient non-uniform flow field. The structure can be either rigid or flexible, straight or curved (including twist) and it can move in an arbitrary manner in an unsteady spatially varying current. It is further assumed in this paper that the surrounding flow field can be studied within a potential realm.

Applications of this problem in nature are abundant and include cases when the structure is composed of liquid particles (such as vortex filaments, Klein & Knio 1995) or bubbles and drops (Longuet-Higgins 1989). Below we mention only a few examples. Starting from the simple case of a rigid structure, one can immediately refer to the important problem of determining the hydrodynamic loading on a straight rigid cylinder embedded in an ambient non-uniform potential flow field (e.g. Lighthill 1986; Rainey 1989 and Chaplin, Rainey & Yemm 1997), which is often encountered in ocean platforms. Then, in order to consider the loading on a closed thin structure (for example, a torus or a helix), one can utilize the results derived for a straight cylinder and extend them to the case of a structure with a curved central line.

Next, by allowing the central line of the cylindrical structure to be time-dependent, it is possible to tackle the stability problem of elastic cable dynamics in a non-uniform ocean environment (see, for example, Zajac 1962) or to determine the spatial shape of an underwater towed cable array used for ocean explorations (Srivastava & Ganapathy 1998). In addition, we are interested in a wide class of hydroelastic problems concerning slender deformable bodies with intrinsic nonlinear elasticity (such as the Kirchhoff rod, Goriely & Tabor 1997) embedded in a potential stream, where the elastics of the structure are combined with the hydrodynamic force distribution.

The reader can be also referred to the problem of fish locomotion (e.g. Taylor 1952 and Lighthill 1960) and a bacterial fibre (Shi & Hearst 1994) or to self-propulsion of a general oscillating deformable surface (Miloh & Galper 1993, Appendix 1). The

https://doi.org/10.1017/S0022112098004170 Published online by Cambridge University Press

hydro-acoustics problem of towed streamers (Dowling 1994), where the temporal variation of the cylinder's central line is of critical importance, should be also mentioned. Yet another challenging problem is the stability of the motion of a viscous liquid jet (deformable and curved) moving in a potential realm (Entov & Yarin 1983), which requires the evaluation of the force distribution along the jet. Finally, it can be noted that the dynamics of a curved vortex filament with a finite core, or the dynamics of two interacting slightly curved vortex filaments (Klein & Knio 1995), depend on the pressure loading on the vortex filament due to the ambient flow field. Such problems require the consideration of the structure with its intrinsic curvature and torsion. In this context we mention for example the helical structures which are often encountered in many different forms from DNA at the molecular level (e.g. Hunt & Hearst 1991), to large twisted vortex filaments (Ricca 1994) at the macro-level.

A slightly different angle of presentation of the force loading exerted on a curved slender structure originates from the problem of finding a suitable modification to the classical form of the Kirchhoff equation governing the motion of a rigid body in an otherwise quiescent fluid (Lamb 1945, § 6), for the case of a deformable body moving arbitrarily in an ambient potential flow field. This problem has been treated over a long period of time by a number of investigators commencing with Taylor (1928), but only recently has a complete solution been given by Galper & Miloh (1995). The formulation is considerably simplified if the body is assumed to be small with respect to the characteristic length of the flow non-uniformity (i.e. weak straining). A question which naturally arises then is how to handle long slender structures where the weakly non-uniform flow assumption may hold only at the cross-sectional plane (i.e. normal to the central line), but definitely not in the direction along the central line. This problem has been extensively studied in the literature (e.g. Lighthill 1986; Manners 1992; Rainey 1995, 1989; Galper, Miloh & Spector 1996) in the context of estimating the wave loads acting on fixed rigid slender straight ocean structures. The motivation for these studies was the timely need to introduce consistent higher-order diffraction inertia terms (beyond the Morison approximation) for a large-diameter vertical cylinder, in order to analyse nonlinear wave phenomena such as springing or ringing (Faltinsen, Newman & Vinje 1995; Malenica & Molin 1995; Chaplin *et al.* 1997). In these papers the ratio between the radius of the cross-section of the structure and the characteristic scale of the non-uniformity of the ambient flow field is treated as a small parameter. At the leading-order (the so-called limit of a 'hydrodynamic line') an exact formula for the loading per unit length, acting on the structure is derived, leading to the important three-dimensional correction to the two-dimensional slender body theory. This is often referred to as the 'axial flow divergence' (Rainey 1995 and Galper *et al.* 1996). A further extension to a stationary vertical large structure with a variable (conical) cross-section, commonly found in an ice infested ocean environment, is given by Galper & Miloh (1997).

The purpose of this work is to present a new concise analysis of the hydrodynamic loads exerted on a slender deformable curved three-dimensional cylindrical structure with an arbitrary cross-section moving in a time-dependent spatially non-uniform ambient potential flow field. One of the important results obtained is an analytic expression for the hydrodynamic load distribution (i.e. the force per unit length) acting on a flexible or rigid long structure in terms of the spatial derivatives of the imposed flow field. The motion of the central line can be either prescribed or coupled with that of the surrounding flow and formulated as a combined hydroelastic problem (fluid–elastic structure interaction).

We employ here a natural intrinsic reference frame (generalized Frenet frame lead-

https://doi.org/10.1017/S0022112098004170 Published online by Cambridge University Press

ing to Lagrangian model coordinates), attached to a curved smooth time-dependent centreline. A rigorous theory of perturbation is then developed based on the assumption that the cross-sectional radius of the structure is small compared with the typical length scale of the ambient flow field non-uniformity. Employing the formalism of Galper & Miloh (1995, § 2), it is demonstrated that instead of the complicated direct method of pressure integration, one can obtain to leading order a rather simplified analytic expression for the force distribution along the central line in terms of the local (two-dimensional) added-mass tensor and the flow gradients evaluated on the central line. A detailed rigorous theoretical investigation of the asymptotic limiting procedure by which the two-dimensional surface is shrunk towards an effectively one-dimensional (hydrodynamic) line, is also given.

The outline of the paper is as follows. In § 2 we consider the hydrodynamic loads acting on a curved slender cylinder of arbitrary cross-section moving in a non-uniform ambient flow field. The expressions for the loading are given in terms of a two-dimensional tensor $\hat{\boldsymbol{m}}$ having the physical sense of a distribution of a three-dimensional added-mass tensor for the cylinder along its central line. In § 3 this distribution is further simplified for the 'hydrodynamic line' limit, i.e. in the limit where the three-dimensional structure is treated as an effectively one-dimensional line (see the Appendix). For this case asymptotic expressions are also obtained. The physical force distribution acting on an arbitrary general curved cylinder which is embedded in a weakly non-uniform ambient flow field is next derived in § 4 and § 5. In § 6 the expression for the force distribution is further extended for deformable cylindrical structures with a time-dependent central line. Finally, we also discuss in § 6 some new applications of this theory to the self-propulsion problem of a deformable thin helix by considering the finite deformations of its central line.

2. Slender cylindrical body with curved central line

2.1. *Weakly non-uniform approximation*

Consider a deformable slender structure with a curved time-dependent smooth central line $C(t)$ of an arbitrary cross-section S. The equation of the centreline is given in terms of its curvature κ, torsion τ and the arclength s measured along the centreline as

$$\kappa = \kappa(s,t), \quad \tau = \tau(s,t). \tag{2.1}$$

We also denote by $T_{\pm}$ the upper and the lower bases of the cylinder respectively and by $2H$ its total length. Thus, the total surface $L(t)$ of the cylinder is given by $L(t) = (C(t) \times S) \cup T_{\pm}$. It is well known (see, for example, Novikov & Fomenko 1980) that (2.1) defines the time-dependent centreline of the cylinder up to rigid motions in three-dimensional space. The cylinder is placed in a non-uniform ambient unsteady potential stream

$$\boldsymbol{V}(\boldsymbol{x},t) = \nabla\phi(\boldsymbol{x},t), \tag{2.2}$$

where $\boldsymbol{x}$ is the position vector in a laboratory coordinate system. The central line of the cylinder can move in an arbitrary manner. The derivation is based on the general methodology recently developed by Galper *et al.* (1996).

The total velocity potential φ, induced by the presence of the moving body, can be uniquely decomposed into two parts:

$$\varphi = \phi + \phi_0, \tag{2.3}$$

https://doi.org/10.1017/S0022112098004170 Published online by Cambridge University Press

where ϕ (harmonic inside L) is the ambient velocity potential and ϕ_0 (harmonic outside L) denotes the additional disturbance potential (Galper & Miloh 1995).

Let us introduce the outer Green function $G(\boldsymbol{x}, \boldsymbol{y}, t)$ for the cylinder

$$\nabla^2 G(\boldsymbol{x}, \boldsymbol{y}, t) = 4\pi\delta(\boldsymbol{x} - \boldsymbol{y}) \tag{2.4}$$

with the corresponding boundary conditions on both L and infinity

$$\frac{\partial}{\partial n(x)} G(\boldsymbol{x}, \boldsymbol{y}, t)\bigg|_{\boldsymbol{x}\in L} = 0, \quad \lim_{|\boldsymbol{x}|\to\infty} G(\boldsymbol{x}, \boldsymbol{y}, t) = 0. \tag{2.5}$$

One can then express ϕ_0 in an integral form as

$$\phi_0(\boldsymbol{x}, t) = -\int_L G(\boldsymbol{x}, \boldsymbol{y}, t)(\boldsymbol{V}\cdot\boldsymbol{n})(\boldsymbol{y})\,\mathrm{d}L(\boldsymbol{y}), \tag{2.6}$$

where $\boldsymbol{n} = \boldsymbol{n}(\boldsymbol{y}, t)$ denotes a unit normal vector to L directed outward into the fluid.

The total hydrodynamic force $\boldsymbol{F}$ acting on a fixed rigid body can be written (see Galper & Miloh 1995) as

$$\boldsymbol{F}(\phi) = \int_L \left(\phi_0 \frac{\partial \boldsymbol{V}}{\partial n} + \boldsymbol{n}\frac{\partial \phi_0}{\partial t}\right)\,\mathrm{d}L + \int_v \left(\frac{\partial \boldsymbol{V}}{\partial t} + (\boldsymbol{V}\cdot\nabla)\boldsymbol{V}\right)\,\mathrm{d}v, \tag{2.7}$$

where $\int_v$ represents a three-dimensional integral over the volume (interior) of the body.

For the case of a deformable body (central line varying with time) (2.7) should be augmented by an additional force loading $\boldsymbol{F}^{(def)}$ arising from the body's pure deformation (Galper & Miloh 1995)

$$\boldsymbol{F}^{(def)} = \int_L \phi^{(d)} \frac{\partial \boldsymbol{V}}{\partial n}\,\mathrm{d}L + \frac{\delta}{\delta t}\int_L \boldsymbol{n}\phi_0\,\mathrm{d}L, \tag{2.8}$$

where $\phi^{(d)}$ is the corresponding deformation potential and $\delta/\delta t$ denotes the time-derivative resulting only from the deformation of the body. The deformation potential $\phi^{(d)}$ can be expressed in terms of the Green function (2.4) as

$$\phi^{(d)}(\boldsymbol{x}, t) = \int_L G(\boldsymbol{x}, \boldsymbol{y}, t)\; V^{(d)}(\boldsymbol{y}, t)\,\mathrm{d}L(\boldsymbol{y}), \tag{2.9}$$

where $V^{(d)}(\boldsymbol{y}, t)$ denotes the deformation velocity of the surface (see Miloh & Galper 1993).

Consider next the case where the characteristic length scale l of the non-uniformity of the ambient flow field $\boldsymbol{V}$ is much larger than the characteristic length scale $|S|$ of the body's cross-section (the so-called 'weakly non-uniform' field approximation). In this case, there exists a small parameter

$$\epsilon \sim \frac{|S|}{l} \ll 1. \tag{2.10}$$

It is important to emphasize here that (2.7) does not actually represent the integration along the central line of the physical force distribution $\bar{\boldsymbol{F}}(z)$ (i.e. the force per unit length) acting on the cross-section. Hence, it is necessary first to modify (2.7) (up to leading-order terms in ϵ) in order to determine the actual force loading per unit length on the cylinder.

https://doi.org/10.1017/S0022112098004170 Published online by Cambridge University Press

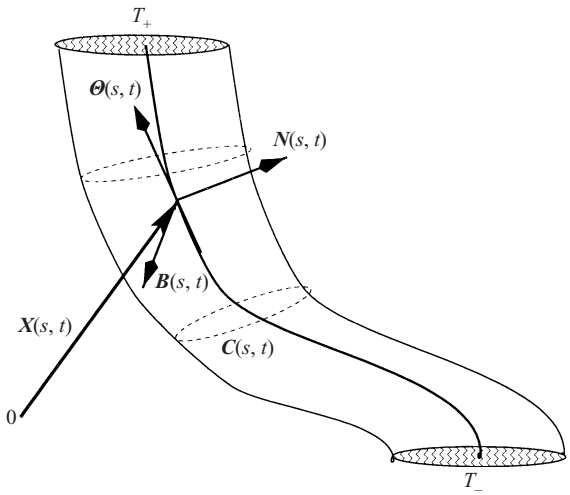


FIGURE 1. A deformable cylinder with a curved time-dependent central line $C(s,t)$. The Frenet triad $\{\Theta(s,t), N(s,t), B(s,t)\}$ is attached to the central line.

2.2. *Generalized coordinates*

To describe the kinematics of the curved central line $C(t)$ it is convenient to introduce a non-orthogonal coordinate system $\{x_1 = s, x_2 = y, x_3 = z\}$ induced by the Frenet triad attached to the curved central line $C(t)$ of the cylinder. Let us write the position vector $\boldsymbol{R}(t)$ of a point on the surface L as

$$\boldsymbol{R} = \boldsymbol{X}(s,t) + y\boldsymbol{N}(s,t) + z\boldsymbol{B}(s,t), \tag{2.11}$$

where $\boldsymbol{X}(s,t)$ represents the position vector of a point on the central line $C(t)$, $\{\boldsymbol{N}, \boldsymbol{B}\}$ denote the normal and bi-normal respectively and s is the natural parameter (arclength) for $C(t)$ (see figure 1). Using the following Frenet differential equations (see Novikov & Fomenko 1990):

$$\frac{\partial \boldsymbol{X}}{\partial s} = \Theta, \quad |\Theta| = 1, \quad \frac{\partial \Theta}{\partial s} = \kappa \boldsymbol{N}, \quad \frac{\partial \boldsymbol{N}}{\partial s} = -\kappa\Theta + \tau\boldsymbol{B}, \quad \frac{\partial \boldsymbol{B}}{\partial s} = -\tau\Theta, \tag{2.12}$$

one can derive the following fundamental matrix g^{ij}:

$$g^{ij} = \frac{1}{(1-\kappa y)^2} \begin{vmatrix} 1 & \tau z & -\tau y \\ \tau z & (1-\kappa y)^2 + \tau^2 z^2 & -\tau^2 yz \\ -\tau y & -\tau^2 yz & (1-\kappa y)^2 + \tau^2 y^2 \end{vmatrix}. \tag{2.13}$$

Using (2.6) and letting $\partial/\partial n \equiv n^{(\alpha)}\nabla_\alpha$, we next obtain

$$\int_L \phi_0 \, (n^{(\alpha)}\nabla_\alpha)\boldsymbol{V} \, \mathrm{d}L = -\int_{-H}^{H} \mathrm{d}s \int_{-H}^{H} \mathrm{d}\acute{s} \int_S \mathrm{d}\boldsymbol{r} \times \int_S \mathrm{d}\acute{\boldsymbol{r}} \, H_s(s,\boldsymbol{r}) \, H_s(\acute{s},\acute{\boldsymbol{r}}) \, V_\alpha(\acute{s},\acute{\boldsymbol{r}}) \, \nabla_\beta(\boldsymbol{r}) \boldsymbol{V}(s,\boldsymbol{r}) n_\alpha(\acute{s},\acute{\boldsymbol{r}}) G(s,\acute{s};\boldsymbol{r},\acute{\boldsymbol{r}}) n_\beta(s,\boldsymbol{r}), \tag{2.14}$$

where we denote a surface element on the structure as $\mathrm{d}L \equiv \mathrm{d}s \, \mathrm{d}\boldsymbol{r} \, H_s(s,\boldsymbol{r})$ with

$$H_s(s,\boldsymbol{r}) = 1 - \kappa(s) y. \tag{2.15}$$

in the right-hand side of (2.14). Here and further when calculating $\int_L$ we neglect the direct contribution of the integration over the two bases $T_\pm$ of the cylindrical

https://doi.org/10.1017/S0022112098004170 Published online by Cambridge University Press

structure. These additional integrals will be accounted for later in §4. Also, here and in what follows, Greek symbols (α, β, γ) take the values 2, 3. Thus, $V_\alpha(s, \boldsymbol{r})$ represents the two projections of $\boldsymbol{V}(s, \boldsymbol{r})$ on the basis vectors lying in the sth cross-section.

By extracting the product of the rate-of-strain tensor times the ambient velocity out of the integration in (2.14) one obtains, by invoking the weak non-uniformity assumption,

$$\int_L \phi_0\, (n^{(\alpha)}\nabla_\alpha)\boldsymbol{V}\, \mathrm{d}L = -\int_{-H}^{H} \mathrm{d}s \int_{-H}^{H} \mathrm{d}\acute{s} V_\alpha(\acute{s}, \acute{\boldsymbol{r}} = 0)\, \nabla_\beta \boldsymbol{V}(s, \boldsymbol{r} = 0) \times \int_S \mathrm{d}\boldsymbol{r} \int_S \mathrm{d}\acute{\boldsymbol{r}}\, H_s(s, \boldsymbol{r})\, H_s(\acute{s}, \acute{\boldsymbol{r}})\, n_\alpha(\acute{s}, \acute{\boldsymbol{r}})\, G(s, \acute{s}; \boldsymbol{r}, \acute{\boldsymbol{r}})\, n_\beta(s, \boldsymbol{r}) + O(\epsilon^2 \log \epsilon), \quad (2.16)$$

where $\boldsymbol{V}(s, r = 0) \equiv \boldsymbol{V}(\boldsymbol{X}(s, t))$.

One can now define the distribution of the added mass as a 2×2 tensor $m_{\alpha\beta}(s, \acute{s})$:

$$m_{\alpha\beta}(s, \acute{s}) \equiv -\int_S \mathrm{d}\boldsymbol{r} \int_S \mathrm{d}\acute{\boldsymbol{r}}\, H_s(s, \boldsymbol{r})\, H_s(\acute{s}, \acute{\boldsymbol{r}})\, n_\alpha(\acute{s}, \acute{\boldsymbol{r}})\, G(s, \acute{s}; \boldsymbol{r}, \acute{\boldsymbol{r}})\, n_\beta(s, \boldsymbol{r}). \quad (2.17)$$

The real three-dimensional added-mass tensor $\hat{\boldsymbol{M}}_L$ of the cylindrical structure L is related to $\hat{\boldsymbol{m}}(s, \acute{s})$ as

$$\hat{\boldsymbol{M}}_L = \int_{-H}^{H} \mathrm{d}s \int_{-H}^{H} \mathrm{d}\acute{s}; \hat{\boldsymbol{O}}(s)\, \hat{\boldsymbol{M}}(s, \acute{s})\, \hat{\boldsymbol{O}}^{-1}(\acute{s}), \quad (2.18)$$

where the Frenet orthogonal matrix $\hat{\boldsymbol{O}}(s)$ denotes the matrix of rotations of the Frenet basis along the central line and the 3×3 matrix $\hat{\boldsymbol{M}}(s, \acute{s}) \equiv \mathrm{diag}(0, \hat{\boldsymbol{m}}(s, \acute{s}))$. One can then express (2.16) in terms of $\hat{\boldsymbol{m}}_{\alpha,\beta}$ as

$$\int_L \phi_0\, (n^{(\alpha)}\nabla_\alpha)\, \boldsymbol{V}\, \mathrm{d}L = \int_{-H}^{H} \mathrm{d}s \int_{-H}^{H} \mathrm{d}\acute{s} V_\alpha(\acute{s}, \acute{\boldsymbol{r}} = 0)\, m_{\alpha\beta}(s, \acute{s})\, \nabla_\beta \boldsymbol{V}(s, \boldsymbol{r} = 0). \quad (2.19)$$

Next, we compute $m_{\alpha\beta}(s, \acute{s})$ in the limit of the weakly non-uniform flow approximation.

3. Leading-order distribution of the added-mass tensor

Owing to the assumption of the weak non-uniformity of the ambient flow field, the added-mass tensor $m_{\alpha\beta}(s, \acute{s})$ is integrated in (2.19) with slowly varying functions of s. Hence, a natural technique for evaluating the convolution (to leading order) with such functions is to first find the Fourier image in the s-direction, namely

$$\tilde{m}_{\alpha\beta}(k, \acute{s}) = \int_{-H}^{H} \mathrm{d}s\, m_{\alpha\beta}(s, \acute{s})\, \mathrm{e}^{\mathrm{i}ks}, \quad (3.1)$$

and then to substitute its inverse Fourier from the corresponding leading-order Taylor expansion of $\tilde{m}_{\alpha\beta}(k, \acute{s})$ back into the convolution (2.19). Furthermore, we assume that both the curvature and torsion of the structure are small enough (i.e. $\max_s \kappa(s)a = O(\epsilon)$ and $\max_s \tau(s)a = O(\epsilon)$), which corresponds to the general limiting procedure of 'hydrodynamic line', where all parameters are considered as fixed as the cross-section radius a tends to zero (Rainey 1995). Note that we do not impose any restrictions on the s-derivatives of the curvature and torsion of the structure. It can be shown (see the Appendix) that in the above-mentioned 'hydrodynamic line' limit, the following asymptotic relationship holds:

$$\tilde{\hat{\boldsymbol{m}}}(k, \acute{s}) = 2\pi^2 a^2 \hat{\boldsymbol{1}} + O(\epsilon^2 \log \epsilon), \quad (3.2)$$

https://doi.org/10.1017/S0022112098004170 Published online by Cambridge University Press

where $\hat{\mathbf{1}}$ is the two-dimensional unit matrix. Thus, we finally find

$$\hat{\boldsymbol{m}}(s,\acute{s}) = \frac{1}{2\pi}\int_{-\infty}^{\infty} \tilde{\hat{\boldsymbol{m}}}(k,\acute{s})\,\mathrm{e}^{-\mathrm{i}ks}\,\mathrm{d}k = \pi a^2\delta(s-\acute{s})\,\hat{\mathbf{1}} + O(\epsilon^2\log\epsilon). \tag{3.3}$$

This means that the individual planar cross-sections contribute independently to the force distribution, as the hydrodynamic line limit is approached. The same statement also holds for non-circular cross-sections of an arbitrary shape. The proof (omitted here) is based on the comparison theorem (McIver & Evans 1985). The mathematical expression (3.3), generalized for the case of a curved slender structure with an arbitrary cross-section, is given by

$$\hat{\boldsymbol{m}}(s,\acute{s}) = \hat{\boldsymbol{m}}^{(0)}\delta(s-\acute{s}), \tag{3.4}$$

where $\hat{\boldsymbol{m}}^{(0)}$ represents the two-dimensional added-mass tensor of the planar cross-section. Substituting (3.4) into (2.18) renders the following generalization of the well-known 'strip'-theory formula (e.g. Tuck 1992) for the case of a slender structure L with a curved central line:

$$\hat{\boldsymbol{M}}^{(L)} = \int_{-H}^{H} \mathrm{d}s\;\hat{\boldsymbol{O}}(s)\,\hat{\boldsymbol{M}}^{(0)}\,\hat{\boldsymbol{O}}^{-1}(s), \tag{3.5}$$

with $\hat{\boldsymbol{M}}^{(0)} \equiv \mathrm{diag}\;(0,\hat{\boldsymbol{m}}^{(0)})$. For a circular cross-section, (3.5) yields the following form:

$$(M)_{ij}^{(L)} = \sigma P\delta_{ij} - \sigma\int_{-H}^{H} \mathrm{d}s\;\Theta_i(s)\,\Theta_j(s), \tag{3.6}$$

where P is the perimeter of the curve L and σ denotes the area of the cross-section. One immediately concludes that $\mathrm{Tr}(\hat{\boldsymbol{M}}^{(L)})) = 2P\sigma$. Clearly, for any planar curve, the added mass in the direction orthogonal to the plane is $M_{orth} = \sigma P$. Hence, for a planar curve with two mutually orthogonal axes of symmetry one immediately derives

$$\hat{\boldsymbol{M}}^{(L)} = P\sigma\;\mathrm{diag}\;(1,\tfrac{1}{2},\tfrac{1}{2}). \tag{3.7}$$

For the particular case of a torus, this result agrees with Miloh, Weisman & Weihs (1978).

Consider further a helix described by

$$\boldsymbol{X}(s,t) = \left(r_0(t)\cos\frac{s}{(r_0^2+p^2)^{1/2}},\; r_0(t)\sin\frac{s}{(r_0^2+p^2)^{1/2}},\; p(t)\frac{s}{(r_0^2+p^2)^{1/2}}\right), \tag{3.8}$$

with pitch p and radius r_0 of the cylinder on which the helix is inscribed. Using (3.6) and the expression for $\boldsymbol{\Theta}(s) = \partial\boldsymbol{X}/\partial s$ for the helix, one directly finds

$$\hat{\boldsymbol{M}}^{(helix)} = P\sigma\;\mathrm{diag}\left(r_0\kappa_0,\left(1-\frac{r_0\kappa_0}{2}\right),\left(1-\frac{r_0\kappa_0}{2}\right)\right). \tag{3.9}$$

For $\tau_0 = 0$, $\kappa_0 = 1/r_0$, the helix degenerates into a torus and (3.9) reduces to (3.7).

4. The correct force distribution

4.1. *Elimination of the tangential forces acting on the bases*

In this section we modify (2.7), which represents the full force acting on the body, so as to obtain the corresponding expression for the physical pressure distribution to the leading order in ϵ. Applying (2.7) as if it were a physical pressure distribution, we

https://doi.org/10.1017/S0022112098004170 Published online by Cambridge University Press

find some fictitious tangential stresses acting on the bases $T_\pm$ which are given by

$$\boldsymbol{F}_{T_\pm} = \int_{T_\pm} \phi_0 \left(\frac{\partial \boldsymbol{V}}{\partial s} \right) \Big|_{T(\pm H)} \mathrm{d}^2 T, \tag{4.1}$$

where $\mathrm{d}^2 T$ represents the two-dimensional area of $T_\pm$. We also denote by $|_{T(s)}$ the corresponding projection of a vector on the plane normal to $\Theta(s)$. Using the particular geometry of a cylindrical structure, one can interpret these additional forces as those originated from an s-integration of some functions which are full s-derivatives, i.e.

$$\boldsymbol{F}_{\pm T} = \int_{-H}^{H} \frac{\mathrm{d}\boldsymbol{f}(s)}{\mathrm{d}s}\, \mathrm{d}s \Big|_{T(\pm H)}. \tag{4.2}$$

Hence, the correct 'physical' force distribution, denoted here by $\bar{\boldsymbol{F}}(s)$, is connected with $\boldsymbol{F}(s)$ defined in (2.7), by

$$\boldsymbol{F}(s) = \bar{\boldsymbol{F}}(s) + \frac{\mathrm{d}\boldsymbol{f}(s)}{\mathrm{d}s}, \tag{4.3}$$

where the unknown vector-function $\boldsymbol{f}(s)$ will be determined further.

Unfortunately, one cannot take this function $\boldsymbol{f}$ to be simply the right-hand side of (4.1), since the term $\phi_0 \partial \mathbf{V}/\partial s$ cannot be analytically continued from the bases into the volume of the cylinder where ϕ_0 has singularities. Hence, let us proceed in a manner similar to Galper *et al.* (1996). The hydrodynamic moment about the centroid of the structure (the origin of the body-attached coordinate system) is given (see § 2 in Galper & Miloh 1995) by

$$\boldsymbol{M}(\phi) = \int_L \left(\phi_0 \frac{\partial(\boldsymbol{R} \wedge \boldsymbol{V})}{\partial n} + \boldsymbol{R} \wedge \boldsymbol{n}\, \frac{\partial \phi_0}{\partial t} \right) \mathrm{d}L + \int_v \boldsymbol{R} \wedge \frac{\mathrm{D}\boldsymbol{V}}{\mathrm{D}t}\, \mathrm{d}v, \tag{4.4}$$

where $\boldsymbol{R}(s, \boldsymbol{r})$ is the position vector (2.11). We will further use the notation

$$\boldsymbol{R}(s, \boldsymbol{r}) = \boldsymbol{X}(s) + \boldsymbol{r}, \tag{4.5}$$

where $\boldsymbol{X}(s)$ is the position vector of a point on the central line and $\boldsymbol{r}$ is the position vector at the sth cross-section. The full moment (4.4) acting on the body must be also corrected, in a similar manner to (4.3), by including a full s-derivative term of some function $\boldsymbol{C}(s)$, namely,

$$\boldsymbol{M}(s) = \bar{\boldsymbol{M}}(s) + \frac{\mathrm{d}\boldsymbol{C}(s)}{\mathrm{d}s}. \tag{4.6}$$

The physical moment distribution $\bar{\boldsymbol{M}}(s)$ is connected to the physical force distribution $\bar{\boldsymbol{F}}(s)$ by

$$\bar{\boldsymbol{M}}(s) = \boldsymbol{X}(s) \wedge \bar{\boldsymbol{F}}(s), \tag{4.7}$$

which follows from a surface integration of the pressure term p.

We now use (2.7), (4.4) and (4.5) in order to write

$$\boldsymbol{M}(s) = \boldsymbol{X}(s) \wedge \boldsymbol{F}(s) + \boldsymbol{M}^{add}(s), \tag{4.8}$$

where

$$\boldsymbol{M}^{add}(s) \equiv \int_S \phi_0(s, \boldsymbol{r}) \frac{\partial}{\partial n} (\boldsymbol{r} \wedge \boldsymbol{V})\, \mathrm{d}S + O(\epsilon^2 \log \epsilon). \tag{4.9}$$

Based on the definitions (4.2) and (4.6) for the functions $\boldsymbol{f}$ and $\boldsymbol{C}$ respectively, it is

https://doi.org/10.1017/S0022112098004170 Published online by Cambridge University Press

concluded that

$$\boldsymbol{f}(\pm H) = \int_{T_\pm} \phi_0 \left(\frac{\partial \boldsymbol{V}}{\partial s} \right) \Big|_{s=\pm H} \mathrm{d}^2 T_\pm, \tag{4.10}$$

and

$$\boldsymbol{C}(\pm H) = \int_{T_\pm} \phi_0 \, \frac{\partial}{\partial s} \left((\boldsymbol{X}(s) + \boldsymbol{r}) \wedge \boldsymbol{V}(s) \right) \Big|_{s=\pm H} \mathrm{d}^2 T_\pm. \tag{4.11}$$

Next, by comparing (4.10) and (4.11), we find

$$\boldsymbol{C}(s = \pm H) = \boldsymbol{X}(s = \pm H) \wedge \boldsymbol{f}(s = \pm H) + \boldsymbol{l}(s = \pm H), \tag{4.12}$$

where

$$\boldsymbol{l}(s = \pm H) \equiv \int_{\pm T} \mathrm{d}^2 T_\pm \, \phi_0 \left(\boldsymbol{r} \wedge \frac{\partial \boldsymbol{V}}{\partial s} + \boldsymbol{\Theta} \wedge \boldsymbol{V} \right). \tag{4.13}$$

It is also seen that $\boldsymbol{l}(s = \pm H)$ cannot be directly continued into v for any s, because of the singular behaviour of ϕ_0. Thus, we can only imply that (4.12) holds for $\boldsymbol{C}(s)$ and $\boldsymbol{f}(s)$ in the sense that

$$\boldsymbol{C}(s) = \boldsymbol{X}(s) \wedge \boldsymbol{f}(s) + \boldsymbol{l}(s), \tag{4.14}$$

where $\boldsymbol{l}(s)$ is some bounded function depending on the fluid variables (namely $\boldsymbol{V}$ and ϕ_0) which are taken at points of their analyticity, but otherwise do not explicitly depend on s.

Substituting now $\bar{\boldsymbol{F}}(s)$ from (4.3) into (4.7) leads to

$$\bar{\boldsymbol{M}} = \boldsymbol{X} \wedge \boldsymbol{F} - \boldsymbol{X} \wedge \frac{\mathrm{d}\boldsymbol{f}}{\mathrm{d}s}. \tag{4.15}$$

After the substitution of (4.8) into (4.6) one obtains

$$\bar{\boldsymbol{M}} = \boldsymbol{X} \wedge \boldsymbol{F} + \boldsymbol{M}^{add} - \frac{\mathrm{d}\boldsymbol{C}}{\mathrm{d}s}. \tag{4.16}$$

Comparing (4.15) with (4.16) and using (4.14), we finally obtain

$$\boldsymbol{M}^{add}(s) = \boldsymbol{\Theta}(s) \wedge \boldsymbol{f}(s) + \frac{\mathrm{d}\boldsymbol{l}(s)}{\mathrm{d}s}, \tag{4.17}$$

where we recall that $\boldsymbol{\Theta}(s)$ is the tangential unit vector to the central line. The last term on the right-hand side of (4.17) when substituted in (4.3) leads to a second-order s-derivative of a bounded function $\boldsymbol{l}(s)$ and hence results in terms of order ϵ^2 in the force distribution (see Galper *et al.* 1996). Thus, one can neglect the last term on the right-hand side of (4.17) in comparison with the first term. It then follows from (4.17) that

$$\boldsymbol{f}(s)\big|_T = \boldsymbol{M}^{add}(s) \wedge \boldsymbol{\Theta}(s) + O(\epsilon^2 \log \epsilon). \tag{4.18}$$

Let us use now a formula which follows from (2.12) and the expansion of any vector along the Frenet basis

$$\frac{\mathrm{d}\boldsymbol{f}}{\mathrm{d}s}\bigg|_T = \left(\frac{\mathrm{d}\boldsymbol{f}|_T}{\mathrm{d}s} \right) \bigg|_T + \kappa f_\Theta \, \boldsymbol{N}, \tag{4.19}$$

where $f_\Theta \equiv \boldsymbol{f} \cdot \boldsymbol{\Theta}$ denotes the tangential component of the vector $\boldsymbol{f}$. We can rewrite (4.3) using 4.19 as

$$\bar{\boldsymbol{F}}(s)\big|_T = \boldsymbol{F}(s)\big|_T - \frac{\mathrm{d}\left(\boldsymbol{f}|_T(s)\right)}{\mathrm{d}s}\bigg|_T - \kappa f_\Theta \, \boldsymbol{N}, \tag{4.20}$$

where the curvature appears explicitly in the last term.

https://doi.org/10.1017/S0022112098004170 Published online by Cambridge University Press

4.2. *The elimination of the tangential forces acting on the face cylinder*

One can then directly determine f_Θ up to $O(1)$ by noticing that, by virtue of (2.16), there exist some fictitious tangential forces acting on the face cylinder, i.e. on the cylinder without its bases.

These non-physical forces $F_\Theta(s)$ can be corrected with the help of $\boldsymbol{f}(s)$ and using (2.12) as

$$\int_{-H}^{H} \mathrm{d}s\, F_\Theta(s)\, \Theta(s) = \int_{-H}^{H} \mathrm{d}s\, \frac{\partial}{\partial s}\left(f_\Theta(s)\, \Theta(s)\right) = \int_{-H}^{H} \mathrm{d}s\, \left(\frac{\partial f_\Theta(s)}{\partial s}\right)\, \Theta(s) + O(\kappa a). \tag{4.21}$$

Note that the product $f_\Theta(s = \pm H)\Theta(s = \pm H)$ has the meaning of a pointed 'response' pressure acting on the bases in the normal direction (see Galper *et al.* 1996, § 8). Using further (2.7) and (3.3) one obtains

$$\begin{aligned} F_\Theta(s) = &- \int_{-H}^{H} \mathrm{d}s \int_{-H}^{H} \mathrm{d}\acute{s} V_\alpha(\acute{s}, \acute{\boldsymbol{r}} = 0)\, \nabla_\beta(s) V_\Theta(s, \boldsymbol{r} = 0) \int_S \mathrm{d}\boldsymbol{r} \int_S \mathrm{d}\acute{\boldsymbol{r}} \\ &\times H_s(s, \boldsymbol{r})\, H_s(\acute{s}, \acute{\boldsymbol{r}})\, n_\alpha(\acute{s}, \acute{\boldsymbol{r}})\, G(s, \acute{s}; \boldsymbol{r}, \acute{\boldsymbol{r}})\, n_\beta(s, \boldsymbol{r}) \\ = &\ \pi a^2 \int_{-H}^{H} \mathrm{d}s\, V_\alpha(s, \acute{\boldsymbol{r}} = 0)\, \nabla_\alpha(s)\, V_\Theta(s, \boldsymbol{r} = 0) \\ = &\ \frac{\pi a^2}{2} \int_{-H}^{H} \mathrm{d}s\, \frac{\partial}{\partial s}\left(V_\alpha(s, \boldsymbol{r} = 0)\, V_\alpha(s, \boldsymbol{r} = 0)\right) + O(\kappa a), \end{aligned} \tag{4.22}$$

where we use

$$\nabla_\alpha V_\Theta(s, \boldsymbol{r} = 0) = \frac{\partial}{\partial s} V_\alpha + O(\kappa a). \tag{4.23}$$

Hence, to leading order (i.e. up to $O(1)$) one obtains

$$f_\Theta(s) = \frac{\pi a^2}{2} \left(\boldsymbol{V}\big|_T\right)^2 (s, \boldsymbol{r} = 0). \tag{4.24}$$

For a non-circular cylinder one obtains by using (3.4) and similarly to (4.20)–(4.24)

$$\boldsymbol{f}_\Theta(s) = \frac{m^{(0)}_{\alpha\beta} V_\alpha V_\beta}{2}, \tag{4.25}$$

which together with (4.20), (4.18) and (4.25) enables us to uniquely determine $\bar{\boldsymbol{F}}(s)$ up to the leading order.

The correct physical force distribution is then obtained from (2.7) and (4.3) as

$$\begin{aligned} \bar{\boldsymbol{F}}(s)\big|_T = &\int_{-H}^{H} \mathrm{d}\acute{s}\, m_{\alpha\beta}(s, \acute{s})\, \left(V_\alpha(\acute{s}, \acute{\boldsymbol{r}} = 0)\, \nabla_\beta\right)\, \boldsymbol{V}(s, \boldsymbol{r} = 0)\big|_T \\ &+ \int_{-H}^{H} \mathrm{d}\acute{s}\, \hat{m}(s, \acute{s}) \frac{\partial \boldsymbol{V}(\acute{s}, \acute{\boldsymbol{r}} = 0)|_T}{\partial t} \\ &+ \sigma \frac{\mathrm{D}\boldsymbol{V}}{\mathrm{D}t}(s, \boldsymbol{r} = 0)\big|_T + \frac{\partial}{\partial s}\left(\boldsymbol{M}^{add}(s) \wedge \boldsymbol{\Theta}(s)\right)\big|_T \\ &- \frac{\kappa(s)}{2} m^{(0)}_{\alpha\beta} V_\alpha V_\beta\, \boldsymbol{N}(s). \end{aligned} \tag{4.26}$$

https://doi.org/10.1017/S0022112098004170 Published online by Cambridge University Press

In deriving (4.26), we employ the following substitution for the last integral in (2.7):

$$\int_{-H}^{H} \mathrm{d}s \int_{\sigma} \frac{\mathrm{D}\boldsymbol{V}}{\mathrm{D}t}(\boldsymbol{r},s)\,\mathrm{d}^2\boldsymbol{r} = \int_{-H}^{H} \mathrm{d}s \frac{\mathrm{D}\boldsymbol{V}}{\mathrm{D}t}(0,s) \int_{\sigma} (1-\kappa(s)y)\,\mathrm{d}^2\boldsymbol{r} = \sigma \int_{-H}^{H} \mathrm{d}s\, \frac{\mathrm{D}\boldsymbol{V}}{\mathrm{D}t}(\boldsymbol{r}=0,s), \tag{4.27}$$

where σ denotes the area of the cross-section and recalling that $\int_{\sigma} y\,\mathrm{d}^2\boldsymbol{r} = 0$.

5. The force distribution on a curved cylinder

Substituting (3.4) into (2.19) one finds in the limit of the hydrodynamic line that

$$\int_{-H}^{H} \mathrm{d}s\ \phi_0\ ((n_\alpha \nabla_\alpha)\boldsymbol{V})\big|_T = \int_{-H}^{H} \mathrm{d}s\,(V_\alpha\, m^{(0)}_{\alpha\beta}\nabla_\beta)\left(\boldsymbol{V}(s)\big|_T\right), \tag{5.1}$$

since $(\nabla_\alpha \boldsymbol{V}(s))\big|_T = (\nabla_\alpha)\left(\boldsymbol{V}(s)\big|_T\right)$. The second integrand on the right-hand side of (2.7) can be written in a similar manner as

$$\int_{L} n_\alpha \frac{\partial \phi_0}{\partial t}\,\mathrm{d}L = \int_{-H}^{H} \mathrm{d}s\, m^{(0)}_{\alpha\beta}\,\frac{\partial V_\beta(s,\boldsymbol{r}=0,t)}{\partial t}. \tag{5.2}$$

Let us next calculate the additional force loading $\boldsymbol{f}(s)$ given by (4.24) and (4.18) in the hydrodynamic line limit (3.3). It can then be shown similarly to (4.24)–(5.2) and by using (3.4) that

$$\mathbf{M}^{add} \wedge \boldsymbol{\Theta}\big|_T = -V_\theta \left(\hat{\boldsymbol{M}}^{(0)}\boldsymbol{V}\right)\big|_T + O(\epsilon^2). \tag{5.3}$$

Next, by gathering (4.19)–(5.3), one finally obtains the following expression for the physical force distribution:

$$\begin{aligned}\bar{\boldsymbol{F}}(s)\big|_T = \sigma \left(\frac{\mathrm{D}\boldsymbol{V}(s)}{\mathrm{D}t}\right)\Bigg|_T + (V_\alpha\, m^{(0)}_{\alpha\beta}\nabla_\beta)\left(\boldsymbol{V}(s)\big|_T\right) + \hat{\boldsymbol{m}}^{(0)}\frac{\partial \boldsymbol{V}|_T}{\partial t} \\ + \left(\left(V_\Theta \frac{\partial}{\partial s}\right)\left(\hat{\boldsymbol{m}}^{(0)}\boldsymbol{V}\big|_T\right)\right)\Bigg|_T + \frac{\partial V_\theta}{\partial s}\left(\hat{\boldsymbol{m}}^{(0)}\boldsymbol{V}\big|_T\right) - \frac{\kappa}{2}(\boldsymbol{V}_T \cdot \hat{\boldsymbol{m}}^{(0)}\boldsymbol{V}_T)\,\boldsymbol{N} + O(\epsilon^2 \log\epsilon).\end{aligned} \tag{5.4}$$

It can be shown that the next order terms on the right-hand side of (5.4) are of $O(\epsilon^2 \log\epsilon)$ (see Galper *et al.* 1996). Equation (5.4) reduces exactly to the expressions recently presented in Rainey (1995) and Galper *et al.* (1996, equations (45), (46)) for the force loading acting on a straight cylinder (i.e. for $\kappa = \tau = 0$).

For a circular cross-section $m^{(0)}_{\alpha\beta} = \sigma\delta_{\alpha\beta}$ and (5.4) can be further simplified to

$$\begin{aligned}\bar{\boldsymbol{F}}(s)\big|_T = \sigma \left(\frac{\mathrm{D}\boldsymbol{V}(s)}{\mathrm{D}t}\right)\Bigg|_T + \sigma(V_\alpha\nabla_\alpha)\left(\boldsymbol{V}(s)\big|_T\right) + \sigma\frac{\partial \boldsymbol{V}|_T}{\partial t} + \sigma\left(\left(V_\Theta\frac{\partial}{\partial s}\right)\left(\boldsymbol{V}\big|_T\right)\right)\Bigg|_T \\ + \sigma\frac{\partial V_\theta}{\partial s}\boldsymbol{V}\big|_T - \sigma\frac{\kappa}{2}(\boldsymbol{V}_T\cdot\boldsymbol{V}_T)\,\boldsymbol{N} + O(\epsilon^2\log\epsilon).\end{aligned} \tag{5.5}$$

It can be also written in a slightly different form. First, by using (4.19) one derives

$$(V_\alpha\nabla_\alpha)\left(\boldsymbol{V}\big|_T(s)\right) + \frac{\partial \boldsymbol{V}}{\partial t}\Bigg|_T + \left(\left(V_\Theta\frac{\partial}{\partial s}\right)\left(\boldsymbol{V}\big|_T\right)\right)\Bigg|_T = \left(\frac{\mathrm{D}\boldsymbol{V}(s)}{\mathrm{D}t}\right)\Bigg|_T - \kappa V_\Theta^2\,\boldsymbol{N}, \tag{5.6}$$

where the substantial time-derivative operator is defined as

$$\frac{\mathrm{D}}{\mathrm{D}t} \equiv \frac{\partial}{\partial t} + V_\alpha\nabla_\alpha + \frac{V_\Theta(s)}{1-\kappa(s)y}\frac{\partial}{\partial s}. \tag{5.7}$$

https://doi.org/10.1017/S0022112098004170 Published online by Cambridge University Press

It is further remarked that one can replace $\mathrm{D}/\mathrm{D}t$ by

$$\frac{\mathrm{D}(s)}{\mathrm{D}t} = \frac{\partial}{\partial t} + V_\alpha \nabla_\alpha + V_\Theta \frac{\partial}{\partial s} + O(\epsilon^2), \tag{5.8}$$

due to the fact that in the limit of a hydrodynamic line, the operator $\mathrm{D}/\mathrm{D}t$ is actually applied on the central line (i.e. for $y = z = 0$). The force loading (5.4) can then be expressed for a circular cylinder in a more compact form in terms of the ambient fluid acceleration $\boldsymbol{a} \equiv \mathrm{D}\boldsymbol{V}/\mathrm{D}t$, by combining (5.6) and (5.8), as

$$\bar{\boldsymbol{F}}(s)\big|_T = 2\sigma \boldsymbol{a}\big|_T + \sigma \frac{\partial V_\theta}{\partial s} \boldsymbol{V}\bigg|_T - \frac{\sigma\kappa}{2}(|\boldsymbol{V}|^2 + V_\Theta^2)\, \boldsymbol{N} + O(\epsilon^2 \log \epsilon). \tag{5.9}$$

Expressed in component form on the Frenet basis, (5.9) also reads

$$F_N(s) = 2\sigma a_N + \sigma \frac{\partial V_\theta}{\partial s} V_N - \frac{\sigma\kappa}{2}(|\boldsymbol{V}|^2 + V_\Theta^2) + O(\epsilon^2 \log \epsilon), \tag{5.10}$$

$$F_B(s) = 2\sigma a_B + \sigma \frac{\partial V_\theta}{\partial s} V_B + O(\epsilon^2 \log \epsilon). \tag{5.11}$$

Thus, one concludes that in the limit of a hydrodynamic line, the curvature of the structure contributes directly to the force distribution only through the last terms on the right-hand side of (5.10) and (5.11). These terms have the physical sense of a central-attraction force. It is also shown that the torsion of the structure does not directly contribute to the force distribution and it is accounted for only indirectly through the varying orientation of the corresponding cross-section planes. It is important to emphasize here that the total force acting on a straight structure in a uniform flow field (i.e. $\boldsymbol{a} = 0$) is always equal to zero. However, for a non-straight central line there exists a non-zero force distribution. One obtains next (using the Frenet equations (2.12)) that for a uniform flow field $\partial V_\theta/\partial s = \kappa V_N$. Thus, for a uniform flow field (5.9) takes the following form:

$$\bar{\boldsymbol{F}}(s)\big|_T = \sigma\kappa \left(V_N \boldsymbol{V}\big|_T - \tfrac{1}{2}(|\boldsymbol{V}|^2 + V_\Theta^2)\, \boldsymbol{N} \right) + O(\epsilon^2 \log \epsilon). \tag{5.12}$$

For a rigid cylindrical structure moving with a velocity $\boldsymbol{U}(t)$, yet an additional force loading arises (see Galper *et al.* 1996, § 6). This additional force distribution can be simply obtained based on the Galilean principle by rewriting (5.9) in a coordinate system moving with the constant velocity $\boldsymbol{U}$. Thus, by replacing $\boldsymbol{V}$ in (5.9) by $\boldsymbol{V} - \boldsymbol{U}$ and $V_\Theta(s)$ by $V_\Theta(s) - U_\Theta(s)$, where $U_\Theta(s) \equiv \boldsymbol{U} \cdot \boldsymbol{\Theta}$ (without altering $\boldsymbol{a}$), we finally obtain

$$\begin{aligned} \bar{\boldsymbol{F}}(s)\big|_T = {} & 2\sigma \boldsymbol{a}\big|_T + \sigma \frac{\partial V_\theta}{\partial s}(\boldsymbol{V} - \boldsymbol{U}) \\ & + \sigma\kappa U_N (\boldsymbol{V} - \boldsymbol{U})\big|_T - \frac{\sigma\kappa}{2}(|\boldsymbol{V} - \boldsymbol{U}|^2 + (V_\Theta - U_\Theta)^2)\, \boldsymbol{N} + O(\epsilon^2 \log \epsilon). \end{aligned} \tag{5.13}$$

In deriving (5.13) we used that $\partial U_\theta/\partial s = \kappa U_N$. For $\kappa = 0$ and $\tau = 0$ (straight rigid cylinder) we recover (56) and (57) of Galper *et al.* (1996).

6. Force distribution due to a deforming central line

6.1. *General formula*

In this section we consider the general motion of a deformable structure with a time-dependent central line $C(s, t)$. Let us denote the deformation velocity of a point

https://doi.org/10.1017/S0022112098004170 Published online by Cambridge University Press

s on $C(s,t)$ by $\boldsymbol{U}^{(d)}(s,t)$. Clearly, for a structure with a fixed centroid location and fixed directions of its main axes (see Miloh & Galper 1993)

$$\boldsymbol{U}^{(d)}(s,t) = \frac{\partial \boldsymbol{X}(s,t)}{\partial t}. \tag{6.1}$$

Note that the deformation velocity is connected with the time- and s-derivatives of the curvature and torsion by the corresponding partial differential equation (see, for example, Ricca 1994). The normal (to the cylindrical structure L) component of this deformation velocity is given by

$$V^{(d)}(s,\boldsymbol{r},t) = \boldsymbol{n}(s,\boldsymbol{r},t)\cdot \boldsymbol{U}^{(d)}(s,t), \tag{6.2}$$

where $\boldsymbol{n}(s,\boldsymbol{r},t)$ is the outward normal to the surface. Substituting (6.2) into (2.8) and using (2.9) leads in the hydrodynamic line limit (compare with (2.19)) to

$$\int_L \phi^{(d)}\,\frac{\partial \boldsymbol{V}}{\partial n}\,\mathrm{d}L = -\int_{-H}^{H}\mathrm{d}s\int_{-H}^{H}\mathrm{d}\acute{s}\; V_\alpha^{(d)}(\acute{s},t)\,m_{\alpha\beta}(s,\acute{s})\nabla_\beta \boldsymbol{V}(s,\boldsymbol{r}=0). \tag{6.3}$$

Choosing to express the leading order of $m_{\alpha\beta}(s,\acute{s})$ in the form of (3.3), one obtains

$$\int_L \phi^{(d)}\,\frac{\partial \boldsymbol{V}}{\partial n}\,\mathrm{d}L = -\sigma\int_{-H}^{H}\mathrm{d}s\left(U_\alpha^{(d)}(s)\nabla_\alpha\right)\boldsymbol{V}(s,\boldsymbol{r}=0). \tag{6.4}$$

The last term on the right-hand side of (2.8) reads to leading order (using (2.9) and (3.3))

$$\begin{aligned}\frac{\delta}{\delta t}\int_L \boldsymbol{n}\phi_0\,\mathrm{d}L &= \sigma\int_{-H}^{H}\mathrm{d}s\,\frac{\delta \boldsymbol{V}(\boldsymbol{X}(s,t))}{\delta t}\\ &= \sigma\int_{-H}^{H}\mathrm{d}s\left(\frac{\partial \boldsymbol{X}}{\partial t}\cdot\nabla_X\right)\boldsymbol{V}(\boldsymbol{X}(s,t)) = \sigma\int_{-H}^{H}\mathrm{d}s\,\left(\boldsymbol{U}^{(d)}(s,t)\cdot\nabla_X\right)\boldsymbol{V}(\boldsymbol{X}(s,t)).\end{aligned} \tag{6.5}$$

Combining (6.4) and (6.5) we derive

$$\int_L \phi^{(d)}\,\frac{\partial \boldsymbol{V}}{\partial n}\,\mathrm{d}L + \frac{\delta}{\delta t}\int_L \boldsymbol{n}\phi_0\,\mathrm{d}L = \sigma\int_{-H}^{H}\mathrm{d}s\;U_\Theta^{(d)}\frac{\partial \boldsymbol{V}}{\partial s}. \tag{6.6}$$

It can be further shown, in a manner similar to (4.1)–(4.17), that the correction vector $\boldsymbol{f}^{(d)}(s)$ which accounts for the deformation is given by

$$\boldsymbol{f}^{(d)}\big|_T = \left(\int_S \phi^{(d)}\,\frac{\partial(\boldsymbol{r}\wedge\boldsymbol{V})}{\partial \boldsymbol{n}}\,\mathrm{d}s\right)\wedge\boldsymbol{\Theta}(s) + O(\epsilon^2), \tag{6.7}$$

which can be further reduced in the hydrodynamic line limit to

$$\boldsymbol{f}^{(d)}\big|_T = -\sigma V_\Theta\,\boldsymbol{U}^{(d)}\big|_T. \tag{6.8}$$

Proceeding next along the same lines as (4.20)–(4.24), one derives

$$\begin{aligned}f_\Theta^{(d)} &= -\sigma\int_{-H}^{H}\mathrm{d}s\;U_\alpha^{(d)}(s)\;\nabla_\alpha(s)V_\Theta(s,\boldsymbol{r}=0)\\ &= -\sigma\int_{-H}^{H}\mathrm{d}s\;\frac{\partial}{\partial s}\left(U_\alpha^{(d)}(s)V_\alpha(s,\boldsymbol{r}=0)\right) + O(\epsilon),\end{aligned} \tag{6.9}$$

where, in deriving (6.9), we used that $\partial U_\alpha(s)/\partial s = O(\epsilon)$. Thus, (6.9) finally reduces to

$$f_\Theta^{(d)} = -\sigma\,\boldsymbol{U}^{(d)}\big|_T\cdot\boldsymbol{V}\big|_T + O(\epsilon). \tag{6.10}$$

https://doi.org/10.1017/S0022112098004170 Published online by Cambridge University Press

Summarizing (6.4)–(6.10) and using (4.19), we conclude therefore that the additional loading per unit length exerted on a curved slender structure due to its own deformation, can be written as

$$\bar{\boldsymbol{F}}^{(d)}(s)\big|_T = \sigma\, U_\Theta^{(d)} \frac{\partial \boldsymbol{V}}{\partial s}\bigg|_T - \sigma\, \frac{\partial}{\partial s}\left(V_\Theta(s)\boldsymbol{U}^{(d)}(s)\big|_T\right)\Big|_T + \sigma\kappa\left(\boldsymbol{U}^{(d)}(s)\big|_T \cdot \boldsymbol{V}(s)\big|_T\right)\, \boldsymbol{N}. \quad (6.11)$$

In (6.11) the ambient velocity $\boldsymbol{V}(s)$ and its cross-sectional derivatives are all evaluated on the central line of the structure, i.e. $\boldsymbol{V}(s) \equiv \boldsymbol{V}(\boldsymbol{X}(s,t))$, etc. One can also rewrite (6.11), using (4.19), in a slightly different form:

$$\bar{\boldsymbol{F}}^{(d)}(s)\big|_T = \sigma\, U_\Theta^{(d)} \frac{\partial \boldsymbol{V}}{\partial s} - \sigma\, \frac{\partial}{\partial s}\left(V_\Theta(s)\boldsymbol{U}^{(d)}(s)\right)\big|_T + \sigma\kappa(\boldsymbol{U}^{(d)}(s)\cdot \boldsymbol{V}(s))\, \boldsymbol{N}. \quad (6.12)$$

It must be also noted that the total force acting on the slender structure due to pure deformations is given by

$$\boldsymbol{F}^{(d)} = \sigma \int_H^H U_\Theta^{(d)} \frac{\partial \boldsymbol{V}}{\partial s}\bigg|_T \mathrm{d}s + O(\epsilon^2). \quad (6.13)$$

Thus, by combining the forces (5.5) and (6.11) we finally obtain the full force distribution acting on the curved deformable structure:

$$\begin{aligned}\bar{\boldsymbol{F}}(s)\big|_T = {} & 2\sigma \boldsymbol{a}\big|_T + U_\Theta^{(d)} \frac{\partial \boldsymbol{V}}{\partial s}\bigg|_T + \sigma\, V_\Theta(s)\left(\frac{\partial}{\partial s}\left(\boldsymbol{V}(s) - \boldsymbol{U}^{(d)}(s)\right)\big|_T\right)\Big|_T \\ & + \sigma \frac{\partial V_\Theta}{\partial s}(\boldsymbol{V} - \boldsymbol{U}^{(d)})\big|_T - \frac{\sigma\kappa}{2}\left(\left(\boldsymbol{V}\big|_T\right)^2 - 2\boldsymbol{V}\big|_T \cdot \boldsymbol{U}^{(d)}\big|_T\right)\, \boldsymbol{N} + O(\epsilon^2 \log \epsilon).\end{aligned} \quad (6.14)$$

Let us consider next a cylindrical structure L embedded in a stationary ambient flow field. We assume in addition that the deformation of its central line is periodic with a certain eigenfrequency ω (induced, for example, by the inner elasticity of the structure). It is also implied that the amplitude A of the deformation is small, i.e. $A \ll l$, where l is the characteristic length scale of the ambient flow field non-uniformity. Taking the average of (6.12) over one period (denoted here by $\langle \cdot \rangle$), we obtain using (6.1)

$$\left\langle U_\Theta^{(d)} \frac{\partial \boldsymbol{V}}{\partial s} \right\rangle = O(\epsilon^2), \left\langle \frac{\partial V_\Theta(s)}{\partial s} \boldsymbol{U}^{(d)}(s) \right\rangle = O(\epsilon^2), \left\langle V_\Theta(s) \frac{\partial \boldsymbol{U}^{(d)}(s)}{\partial s} \right\rangle = O(\epsilon^2), \quad (6.15)$$

as full time derivatives. Finally, the only term surviving the time averaging is

$$\left\langle \bar{F}_N^{(d)}(s) \right\rangle = -\sigma\left(\langle \kappa(s)\boldsymbol{U}^{(d)}\rangle \cdot \boldsymbol{V}\right)\, \boldsymbol{N} + O(\epsilon^2). \quad (6.16)$$

We do not average $\big|_T$ and $\boldsymbol{N}(t)$ here, because we are interested in the averaged force acting on the same material cross-section. Note that for a small (infinitesimal) deformation the deformational velocity is proportional to the time-derivatives $\dot{\kappa}$ and $\dot{\tau}$ (a result which for a small deformation can be obtained by a Taylor expansion of the deformation velocity). Hence, we conclude that in order to have a non-zero average cross-sectional force, the term $\langle \kappa(\partial(\tau)/\partial t)\rangle$ must be non-zero. Thus, the curvature and torsion deformation modes of the structure L should have some out-of-phase component in order for a persistent cross-sectional loading to exist.

The presence of a finite time-averaged load acting on an elastic structure can lead to a bifurcation of its averaged equilibrium position (Goriely & Tabor 1997). It can

https://doi.org/10.1017/S0022112098004170 Published online by Cambridge University Press

also, in its turn, increase the knottiness of an elastic slender cable embedded in an ambient stream.

6.2. *Self-propulsion of a helix*

We apply here the asymptotic expression (3.9) for the added mass of a helix for analysing the problem of self-propulsion of a deformable helix in a quiescent fluid or for the self-locomotion problem of a bacterial fibre (Shi & Hearst 1994). It is shown that by enforcing a specially prescribed finite periodic deformation of its central line, the helix (3.8) can propel itself with a persistent velocity (time averaged over the period). Following Miloh & Galper (1993), the velocity $\boldsymbol{V}^{(c)}$ of the centroid of a deformable helix L (initially at rest) moving in an otherwise quiescent fluid is given by

$$\boldsymbol{V}^{(c)} = (\rho_b v \hat{\boldsymbol{I}} + \hat{\boldsymbol{M}})^{-1} \int_L \phi^{(d)}\, \boldsymbol{n}\, \mathrm{d}L, \tag{6.17}$$

where ρ_b denotes the density of the body. Proceeding in a similar manner to (6.4), and invoking the hydrodynamic line limiting procedure, (6.17) yields for a circular cross-section

$$\boldsymbol{V}^{(c)} = \sigma(\rho_b v \hat{\boldsymbol{I}} + \hat{\boldsymbol{M}})^{-1} \int_{-H}^{H} \mathrm{d}s\ \ \boldsymbol{U}^{(d)}\big|_{T(s)}. \tag{6.18}$$

Taking the projection of (6.18) on the axis of symmetry of the helix $\boldsymbol{e}_3$ and using (3.9), we derive (see, for example, Ricca 1994)

$$V_3^{(c)} = \frac{1}{P(\rho_b + \kappa r_0)} \int_{-H}^{H} \mathrm{d}s\ \ \boldsymbol{U}^{(d)}\big|_{T(s)} \cdot \boldsymbol{e}_3 = \frac{P}{2(\rho_b + \kappa r_0)} \kappa \frac{\mathrm{d}p}{\mathrm{d}t} \frac{r_0}{(r_0^2 + p^2)^{1/2}}, \tag{6.19}$$

where P is the total perimeter and r_0 and p denote the radius and pitch of the helix respectively. To illustrate the optimal strategy of self-propulsion let us consider the case of a massless body where $\rho_b \ll 1$. After taking the time average, denoted by $\langle \cdot \rangle$, of (6.19) one obtains

$$\left\langle V_3^{(c)} \right\rangle = \frac{P}{2} \left\langle \frac{\mathrm{d}p/\mathrm{d}t}{(r_0^2 + p^2)^{1/2}} \right\rangle = -\frac{P}{2} \left\langle \frac{\mathrm{d}\tau/\mathrm{d}t}{(\tau^2 + \kappa^2)^{1/2}} \right\rangle. \tag{6.20}$$

Equation (6.20) demonstrates (see also the discussion in Miloh & Galper 1993; Shapere & Wilczek 1990; Benjamin & Ellis 1990) that an efficient self-propulsion mechanism must include two mutually skew-symmetric surface modes (i.e. torsion and curvature in our case) with a $\pi/2$ phase shift between them for maximum efficiency.

7. Summary

A rigorous derivation of the formulae for computing the force loading on a three-dimensional cylindrical structure with a curved (finite curvature and torsion) central line is presented in the limit of a hydrodynamic line. In this limit the characteristic length scale of the ambient flow field and also the principal radii of its central line are assumed to be much larger than the radius of the cross-section of the structure. No other restrictions on the geometry of the three-dimensional structure and on the derivatives of its curvature and torsion are imposed.

The construction of the corresponding asymptotic analysis for the outer Green function of the structure is first applied to the problem of determining the added mass of a deformable thin structure. We determine the corresponding extension of

https://doi.org/10.1017/S0022112098004170 Published online by Cambridge University Press

the 'strip theory', known for straight structures with a variable cross-section. As an example, we obtain the asymptotic added masses for an arbitrary thin helix. Based on this, we present a certain type of finite-amplitude self-propulsion mechanism of a deformable helix, which originates from interactions of torsion–curvature modes. This is the first time that an optimal strategy of self-locomotion with non-restricted amplitude of deformation has been proposed.

This mechanism may lead, for example, to a non-trivial persistent cross-sectional loading on a curved vibrating deformable structure, resulting from nonlinear interactions between the curvature and torsion modes coupled with the ambient flow field non-uniformity. This term tends to reduce the force loading on a curved structure compared with that exerted on a straight structure having the same cross-section.

This work was supported by the Israeli Science Foundation, Contract No. 544 222. The partial support from the Ocean Technology Division of ONR (N00014-97-1-0039) is also acknowledged.

Appendix. The added-mass tensor

A.1. *Laplace equation in generalized coordinates*

Let us first express (2.4) in the coordinate system (2.11) using the following expression for the Laplacian in an arbitrary generalized coordinate system (Novikov & Fomenko 1990):

$$\nabla^2\phi = g^{ij}\frac{\partial^2\phi}{\partial x^i x^j} + \frac{1}{|g|^{1/2}}\frac{\partial}{\partial x^j}(|g|^{1/2}g^{ij})\frac{\partial\phi}{\partial x^i}, \tag{A 1}$$

where $|g|$ denotes the determinant of the matrix g^{ij} given by (2.13). One can readily verify, using (2.13) that $|g| = (1-\kappa y)^2$. It is convenient at this stage to introduce polar coordinates r and θ at every cross-section as $y = r\cos\theta$, $z = r\sin\theta$. Direct calculations of the various terms in (A 1) lead to

$$g^{ij}\frac{\partial^2}{\partial x^i x^j} = \Delta_{yz} + \frac{1}{(1-\kappa(s)y)^2}\left(\frac{\partial}{\partial s} + \tau(s)\frac{\partial}{\partial\theta}\right)^2, \tag{A 2}$$

where Δ_{yz} denotes the two-dimensional Laplacian, i.e. $\Delta_{yz} \equiv \left(\partial^2/\partial y^2 + \partial^2/\partial z^2\right)$.

For the second term on the right-hand side of (A 1) one obtains after some tedious calculations

$$\frac{1}{|g|^{1/2}}\frac{\partial}{\partial x^j}\left(|g|^{1/2}g^{ij}\right)\frac{\partial}{\partial x^i} = -\frac{\kappa}{1-\kappa y}\frac{\partial}{\partial y} + \frac{\partial\kappa(s)}{\partial s}\frac{y}{(1-\kappa y)^3}\left(\frac{\partial}{\partial s} + \tau\frac{\partial}{\partial\theta}\right) + \frac{\tau^2 r}{(1-\kappa y)^3}\left(\kappa r\frac{\partial}{\partial y} - \frac{\partial}{\partial r}\right). \tag{A 3}$$

In order to apply (A 1)–(A 3) to the Green function $G(s,\acute{s};\boldsymbol{r},\acute{\boldsymbol{r}})$ expressed now in the generalized coordinates (2.4), we write the δ-function as

$$\delta(\boldsymbol{x}-\acute{\boldsymbol{x}}) = \frac{1}{|g|^{1/2}}\delta(s-\acute{s})\delta(\boldsymbol{r}-\acute{\boldsymbol{r}}), \tag{A 4}$$

where $\boldsymbol{r}$ is the two-dimensional position vector in the cross-section. Combining (A 1)–(A 4) in a single equation replacing (2.4), we finally obtain for the Green function

https://doi.org/10.1017/S0022112098004170 Published online by Cambridge University Press

$G(s,\acute{s};\boldsymbol{r},\acute{\boldsymbol{r}})$;

$$\left(\Delta_{yz}\left((1-\kappa y)\right)+\frac{1}{(1-\kappa(s)y)}\left(\frac{\partial}{\partial s}+\tau(s)\frac{\partial}{\partial\theta}\right)^2\right)G(s,\acute{s};\boldsymbol{r},\acute{\boldsymbol{r}})$$
$$+\left(\frac{\partial\kappa(s)}{\partial s}\frac{y}{(1-\kappa y)^2}\left(\frac{\partial}{\partial s}+\tau\frac{\partial}{\partial\theta}\right)+\frac{\tau^2 r}{(1-\kappa y)^2}\left(\kappa r\frac{\partial}{\partial y}-\frac{\partial}{\partial r}\right)\right)G(s,\acute{s};\boldsymbol{r},\acute{\boldsymbol{r}})$$
$$=4\pi\delta(s-\acute{s})\delta(\boldsymbol{r}-\acute{\boldsymbol{r}}). \tag{A 5}$$

Consider first the particular case of a circular cross-section with a constant radius a (i.e. $S=r-a=0$). The corresponding boundary condition for such a cylinder reads now

$$\frac{\partial}{\partial\boldsymbol{r}}G(s,\acute{s};\boldsymbol{r},\acute{\boldsymbol{r}})\big|_{r=a}=0, \tag{A 6}$$

which is supplemented by demanding a proper exponential decay at infinity.

A.2. *The limit of hydrodynamic line*

It is convenient to denote

$$(1-\kappa y)\,G(s,\acute{s};\boldsymbol{r},\acute{\boldsymbol{r}})\equiv\Gamma(s,\acute{s};r,\acute{r}). \tag{A 7}$$

One can then rewrite (A 5) and (A 6) in terms of Γ using the polar coordinates and the two-dimensional Laplacian $\Delta_{r\theta}$ as

$$\Delta_{r\theta}\Gamma+\frac{1}{(1-\kappa(s)y)^2}\frac{\partial^2\Gamma}{\partial s^2}+\hat{\mathrm{D}}\Gamma=4\pi\delta(s-\acute{s})\delta(\boldsymbol{r}-\acute{\boldsymbol{r}}), \tag{A 8}$$

where the differential operator $\hat{\mathrm{D}}$ is defined by

$$\hat{\mathrm{D}}(s,\boldsymbol{r})=\frac{1}{(1-\kappa y)^2}\left(\tau\frac{\partial^2}{\partial\theta\partial s}+\frac{\partial\tau}{\partial s}\frac{\partial}{\partial\theta}+\tau^2\frac{\partial^2}{\partial\theta^2}\right)+\frac{r\cos\theta}{(1-\kappa y)^3}\frac{\partial\kappa}{\partial s}\left(\frac{\partial}{\partial s}+\tau\frac{\partial}{\partial\theta}\right)$$
$$-\frac{\tau r}{(1-\kappa y)^2}\frac{\partial}{\partial r}-\frac{\tau^2 r\kappa\sin\theta}{(1-\kappa y)^2}\frac{\partial}{\partial\theta}. \tag{A 9}$$

The impermeable boundary condition (A 6) now takes the form

$$\left.\frac{\partial}{\partial r}\Gamma+\frac{\kappa\cos\theta}{1-\kappa y}\Gamma\right|_{r=a}=0. \tag{A 10}$$

Next we apply the operator of Fourier transform $\hat{F}$ in the s-direction to (A 8). Note that, as we will show below, the image of Γ which is denoted here by $\hat{F}\Gamma(s,\acute{s},\boldsymbol{r})\equiv\tilde{\Gamma}(k,\acute{s},\boldsymbol{r},\acute{\boldsymbol{r}})$, has a finite limit for $k\to0$ (i.e. in the limit of the hydrodynamic line) and hence

$$\Gamma(s,\acute{s},\boldsymbol{r},\acute{\boldsymbol{r}})\sim\delta(s-\acute{s})+O(\epsilon^2). \tag{A 11}$$

Correspondingly, $\hat{F}(\hat{\mathrm{D}}\Gamma)=\tilde{\hat{\mathrm{D}}}\tilde{\Gamma}+O(\epsilon^2)$, where the differential operator $\tilde{\hat{\mathrm{D}}}(k,\acute{s},\boldsymbol{r})$ is essentially the same as the operator $\hat{\mathrm{D}}(s,\acute{s},\boldsymbol{r})$, but with $\partial/\partial s$ replaced by k, $\partial\kappa(s)/\partial s$ replaced by $k\kappa(\acute{s})$ and $\partial\tau(s)/\partial s$ by $k\tau(\acute{s})$. Thus, we obtain the following governing equation for $\tilde{\Gamma}$:

$$\left(\frac{\partial^2}{\partial r^2}+\frac{1}{r}\frac{\partial}{\partial r}+\frac{1}{r^2}\frac{\partial^2}{\partial\theta^2}-\frac{k^2}{(1-\kappa y)^2}\right)\tilde{\Gamma}(k,\acute{s},\boldsymbol{r},\acute{\boldsymbol{r}})+\tilde{\hat{\mathrm{D}}}\tilde{\Gamma}(k,\acute{s},\boldsymbol{r},\acute{\boldsymbol{r}})=4\pi\mathrm{e}^{\mathrm{i}k\acute{s}}\delta(\boldsymbol{r}-\acute{\boldsymbol{r}}), \tag{A 12}$$

https://doi.org/10.1017/S0022112098004170 Published online by Cambridge University Press

with the corresponding boundary condition

$$\frac{\partial}{\partial r}\tilde{\Gamma} + \frac{\kappa(\acute{s})\cos\theta}{1-\kappa(\acute{s})a\cos\theta}\tilde{\Gamma}\bigg|_{r=a} = 0, \tag{A 13}$$

where the differential operator $\tilde{\hat{\mathrm{D}}}$ is defined as

$$\tilde{\hat{\mathrm{D}}}(\acute{s},\boldsymbol{r}) = \frac{1}{(1-\kappa(\acute{s})y)^2}\left(2k\tau(\acute{s})\frac{\partial}{\partial\theta} + \frac{k\kappa(\acute{s})(r\tau(\acute{s})\cos\theta)}{1-\kappa(\acute{s})y}\frac{\partial}{\partial\theta}\right.$$
$$\left. +\tau^2(\acute{s})\frac{\partial^2}{\partial\theta^2} - \tau^2(\acute{s})r\kappa(\acute{s})\sin\theta\frac{\partial}{\partial\theta}\right) + \frac{k^2\kappa(\acute{s})r\cos\theta}{(1-\kappa y)^3} - \frac{\tau^2(\acute{s})r}{(1-\kappa y)^2}\frac{\partial}{\partial r}. \tag{A 14}$$

It can be shown that the term $\hat{\mathrm{D}}\tilde{\Gamma}$ can be neglected in comparison with the first term on the left-hand side of (A 12), being of order ϵ^2 at the vicinity of L ($r \sim a$), i.e. just where the convolution limit of (2.16) is located. It is also emphasized that the term proportional to $k^2\tilde{\Gamma}$ is kept in (A 12), so as to guarantee the correct (exponential) decay of $\tilde{\Gamma}$ at infinity.

Let us next define the following Fourier transform:

$$\tilde{\Phi}_\alpha(k,\acute{s},\boldsymbol{r}) \equiv \mathrm{e}^{\mathrm{i}k\acute{s}}\int_S \mathrm{d}\acute{\boldsymbol{r}}\tilde{\Gamma}(k,\acute{s};\boldsymbol{r},\acute{\boldsymbol{r}})n_\alpha(\acute{s},\acute{\boldsymbol{r}}). \tag{A 15}$$

Combining (A 12) (with $\hat{\mathrm{D}} = 0$), (A 13) and (A 15) we obtain

$$\left(\Delta_{r\theta} - k^2\right)\tilde{\Phi}_\alpha(k,\acute{s},\boldsymbol{r}) + O(\epsilon^3) = 0, \tag{A 16}$$

subject to the boundary condition

$$\frac{\partial\tilde{\Phi}_\alpha}{\partial r} + \kappa(\acute{s})\cos\theta\ \tilde{\Phi}_\alpha\big|_{r=a} = \mathrm{e}^{\mathrm{i}k\acute{s}}n_\alpha\big|_{r=a} + O(\epsilon^2). \tag{A 17}$$

In deriving (A 16) and (A 17) we used the expansions

$$\frac{k^2}{(1-\kappa r\cos\theta)^2}\bigg|_{r\sim a} = k^2(1+2\kappa r\cos\theta)\big|_{r\sim a} + O(\epsilon^2), \quad \frac{1}{(1-\kappa a\cos\theta)} = (1+\kappa a\cos\theta) + O(\epsilon^2).$$

We seek a solution of (A 16) decaying at infinity (helped by (A 17)). For say $\alpha = 2$ this solution is expressed in the following form:

$$\tilde{\Phi}_2(k,r,\theta) = \mathrm{e}^{\mathrm{i}k\acute{s}}(A_0(k)K_0(kr) + A_1(k)K_1(kr)\cos\theta + A_2(k)K_2(kr)\cos 2\theta + \cdots), \tag{A 18}$$

where K_n are the corresponding cylindrical Bessel functions of order n.

Only the terms with A_0, A_1 and A_2 survive the integration of (A 18), with the normals in (2.16), which when combined together with (A 15), finally leads to

$$\begin{aligned} m_{22}(s,\acute{s}) &\equiv -\int_S \mathrm{d}\boldsymbol{r}\int_S \mathrm{d}\acute{\boldsymbol{r}}H_s(s,\boldsymbol{r})\ H_s(\acute{s},\acute{\boldsymbol{r}})\ n_2(\acute{s},\acute{\boldsymbol{r}})G(s,\acute{s};\boldsymbol{r},\acute{\boldsymbol{r}})n_2(s,\boldsymbol{r}) \\ &= -\int_S \mathrm{d}\boldsymbol{r}\ (1-a\kappa(\acute{s})\cos\theta)\ \cos\theta\ \hat{F}^{-1}(\tilde{\Phi}_2(\acute{s},k,\boldsymbol{r})) \\ &= 2\pi^2 a\hat{F}^{-1}\left(A_1(k)K_1(ka) - \kappa aA_0(k)K_0(ka) - \frac{\kappa a}{2}A_2(k)K_2(ka)\right) \end{aligned} \tag{A 19}$$

where $\hat{F}^{-1}$ represents the inverse Fourier transform. The distributed two-dimensional added-mass tensor is diagonalized, i.e. $m_{\alpha\beta}(s) = \mathrm{diag}(m_{22}, m_{33})$ with $m_{22} = m_{33}$. Substituting (A 18) in (A 17) leads, after successive integrations with $\cos m\theta$ for $m = 0, 1$

https://doi.org/10.1017/S0022112098004170 Published online by Cambridge University Press

and by keeping only leading-order terms in κa, to

$$A_0 = -\frac{\kappa K_1(ak)}{2k\dot{K}_0(ak)}A_1, \quad A_1 = \frac{1}{k\dot{K}_1(ak)\alpha_1} - \frac{\kappa}{2k\alpha_1}\frac{K_2(ak)}{\dot{K}_1(ak)}A_2, \tag{A 20}$$

where

$$\alpha_1 \equiv 1 - \frac{\kappa^2}{2k^2}\frac{K_0(ak)K_1(ak)}{\dot{K}_0(ak)\dot{K}_1(ak)}. \tag{A 21}$$

The overdot denotes differentiation with respect to the argument.

Using (A 20)–(A 21) we have

$$\left(A_1(k)K_1 - \kappa a A_0(k)K_0 - \frac{\kappa a}{2}A_2(k)K_2\right) = \frac{K_1}{k\dot{K}_1\alpha_1}\left(1 + \frac{\kappa^2 a}{2k}\frac{K_0}{\dot{K}_0}\right) + A_2\frac{\kappa K_2}{2k\alpha_1}\left(\frac{K_1}{\dot{K}_1} + \frac{\kappa^2 K_0 K_1}{2k\dot{K}_0\dot{K}_1} + ka\alpha_1\right) \tag{A 22}$$

where all functions are evaluated at the point ak. Using the following expansions:

$$K_0(kr) = \log(kr) + O(k^2r^2\log kr), \quad K_n(kr) \sim \frac{1}{(kr)^n} + O(k^{n-1}r^{n-1}), \quad n > 0, \tag{A 23}$$

it is found that the term with A_2 in (A 22) is exactly zero (up to leading-order in ak). Indeed, in the limit of a hydrodynamic line, we use

$$\alpha_1(ak) = 1 + \frac{\kappa^2 a^2}{2}\log ka, \quad \frac{K_1(ak)}{\dot{K}_1(ak)} = -ka, \quad \frac{K_0(ak)K_1(ak)}{\dot{K}_0(ak)\dot{K}_1(ak)} = -k^2a^2\log ak \tag{A 24}$$

which nullifies the second parenthesis on the right-hand side of (A 22).

Hence, following (A 23), the only remaining terms in (A 22) are

$$\left(A_1K_1(ka) - \kappa a A_0(k)K_0(ka) - \frac{\kappa a}{2}A_2(k)K_2(ka)\right) = a + O(a^2k^2\log ak). \tag{A 25}$$

Finally, substituting (A 25) into (A 19), we finally obtain (3.2).

REFERENCES

Benjamin, T. B. & Ellis, A. T. 1990 Self-propulsion of asymmetrically vibrating bubbles. *J. Fluid Mech.* **212**, 65–80.

Chaplin, J. R., Rainey, R. C. T. & Yemm R. W. 1997 Ringing of a vertical cylinder in waves. *J. Fluid Mech.* **350**, 119–147.

Dowling, A. P. 1994 Unsteady flow near a moving cylinder. *J. Fluid Mech.* **278**, 363–390.

Entov, M. & Yarin, A. L. 1985 Liquid jet instability. *J. Fluid Mech.* **220**, 141–170.

Faltinsen, O. M., Newman J. N. & Vinje, T. 1995 Nonlinear wave loads on a slender vertical cylinder. *J. Fluid Mech.* **289**, 179–199.

Galper, A. R. & Miloh, T. 1995 Dynamical equations for the motion of a deformable body in an arbitrary potential non-uniform flow field. *J. Fluid Mech.* **295**, 91–120.

Galper, A. R. & Miloh, T. 1997 Hydrodynamic loads on a conical slender cylinder. *J. Offshore Mech. Arctic Engng* **119**, 42–45.

Galper, A. R., Miloh, T. & Spector, M. 1996 Hydrodynamic loads on a cylinder moving unsteadily in a three-dimensional non-uniform flow field. *Appl. Ocean Res.* **18**, 29–36.

Goriely, A. & Tabor, M. 1997 Nonlinear dynamics of filaments I: Dynamical instabilities. *Physica* D **105**, 20–44.

Hunt, N. G. & Hearst, J. E. 1991 Elastic model of DNA supercoiling in the infinite length limit. *J Chem. Phys.* **12**, 9329–9336.

https://doi.org/10.1017/S0022112098004170 Published online by Cambridge University Press

Klein, R. & Knio, O. M. 1995 Asymptotic vorticity structure and numerical simulation of slender vortex filaments. *J. Fluid Mech.* **284**, 275–321.

Lamb, H. 1945 *Hydrodynamics.* Dover.

Lighthill, M. J. 1960 Note on swimming of slender fish. *J. Fluid Mech.* **9**, 305–317.

Lighthill, M. J. 1986 Fundamentals concerning wave loading on offshore structures. *J. Fluid Mech.* **173**, 667–681.

Longuet-Higgins, M. S. 1989 Monopole emission of sound by asymmetric bubble oscillations. Part 2. *J. Fluid Mech.* **201**, 543–565.

Malenica, S. & Molin, B. 1995 Third order wave diffraction by a vertical cylinder. *J. Fluid Mech.* **302**, 203–229.

Manners, W. 1992 Hydrodynamic force on a moving circular cylinder submerged in a general fluid flow. *Proc. R. Soc. Lond.* A **438**, 331–339.

McIver, P. & Evans, D. V. 1985 The trapping of surface waves above a submerged horizontal cylinder. *J. Fluid Mech.* **151**, 243–255.

Miloh, T. & Galper, A. R. 1993 Self-propulsion of a maneuvering deformable body in a perfect fluid. *Proc. R. Soc. Lond.* A **442**, 273.

Miloh, T., Weisman, G. & Weihs, D. 1978 The added-mass coefficient of a torus. *J. Engng Maths* **12**, 1–13.

Novikov, S. P. & Fomenko, A. T. 1990 *Basic Elements of Differential Geometry and Topology.* Kluwer.

Rainey, R. C. T. 1989 A new equation for wave loads on offshore structures. *J. Fluid Mech.* **204**, 295–324.

Rainey, R. C. T. 1995 Slender-body expressions for the wave load on offshore structures. *Proc. R. Soc. Lond.* A **450**, 391–416.

Ricca R. L. 1994 The effect of torsion on the motion of a helical vortex filament. *J. Fluid Mech.* **273**, 241–261.

Shapere, A. & Wilczek, F. 1989 Geometry of self-propulsion at low Reynolds number. *J. Fluid Mech.* **198**, 557–586.

Shi, Y. & Hearst, J. E. 1994 The Kirchhoff elastic rod, the nonlinear Schroedinger equation and DNA supercoiling. *J. Chem. Phys.* **101**, 5186–5194.

Srivastava, S. K. & Ganapathy, C. 1998 Experimental investigation on loop-manoevre of underwater towed cable-array system. *Ocean Engng* **25**, 85–12.

Taylor, G. I. 1928 The forces on a body placed in a curved or converging stream of fluid. *Proc. R. Soc. Lond.* A **120**, 260–283.

Taylor, G. I. 1952 Analysis of a swimming of long and narrow animals. *Proc. R. Soc. Lond.* A **214**, 158–183.

Tuck, E. O. 1992 Analytic aspects of slender body theory. In *Wave asymptotics* (ed. P. Martin & L. Wickham), pp. 184–201. Cambridge University Press.

Zajac, E. E. 1962 Stability of two loop elasticas. *Trans. ASME* 136–142.

https://doi.org/10.1017/S0022112098004170 Published online by Cambridge University Press